

## Light emission from an ambipolar semiconducting polymer field-effect transistor

James S. Swensen<sup>a)</sup>

Department of Materials Sciences, Center for Polymers and Organic Solids, University of California, Santa Barbara, Santa Barbara, California 93106

Cesare Soci

Department of Physics, Center for Polymers and Organic Solids, University of California, Santa Barbara, Santa Barbara, California 93106

Alan J. Heeger<sup>b)</sup>

Department of Materials Sciences, Center for Polymers and Organic Solids, University of California, Santa Barbara, Santa Barbara, California 93106

(Received 22 August 2005; accepted 10 November 2005; published online 15 December 2005)

Ambipolar light-emitting field-effect transistors are fabricated with two different metals for the top-contact source and drain electrodes; a low-work-function metal defining the channel for the source electrode and a high-work-function metal defining the channel for the drain electrode. A thin film of polypropylene-co-1-butene on  $\text{SiN}_x$  is used as the gate dielectric on an  $n^{++}$ -Si wafer, which functioned as the substrate and the gate electrode. Transport data show ambipolar behavior. Recombination of electrons and holes results in a narrow zone of light emission within the channel. The location of the emission zone is controlled by the gate bias. © 2005 American Institute of Physics. [DOI: 10.1063/1.2149986]

Several research groups have published results recently showing light emission within the channel of organic field-effect transistors (FETs), mainly for small molecules<sup>1–6</sup> but with some reports involving semiconducting polymers.<sup>7–10</sup> Generally, the bottom contact device geometry was used with gold as the metal for both the source and the drain electrodes.<sup>1,2,4,5,7</sup> Although light emission was observed near (or even slightly under) the negative drain electrode, these devices showed only hole transport. This is to be expected since electron injection from a high-work-function metal, such as gold, into the organic semiconductor would be limited by a large-energy barrier.

Showing electron transport in polymer FETs had proven difficult until recently. Chua *et al.*<sup>11</sup> determined that hydroxyl groups serve as traps for electrons at the polymer-silicon dioxide ( $\text{SiO}_2$ ) interface in FETs fabricated on Si with  $\text{SiO}_2$  as the gate dielectric. By passivating the  $\text{SiO}_2$  with pure nonpolar polymer dielectrics, electron transport was achieved in various conjugated polymers.

Efficient ambipolar injection in an FET requires the “two-color” electrode geometry, where the channel region of the transistor is defined by a low-work-function metal on one side and a high-work-function metal on the opposite side. Light emission in the channel region of an FET using the two-color electrode geometry was demonstrated.<sup>3,6,8–10</sup> Of those who employed the two-color electrodes, only Rost *et al.*<sup>3</sup> were able to show ambipolar behavior. Yet, the effect of the gate bias on the light emission was left unclear.

In this work, we report a semiconducting polymer light-emitting FET (LEFET) fabricated by employing a new “angled” evaporation technique to deposit top-contact two-

color electrodes. Ambipolar transport was achieved by passivating the gate dielectric in a similar fashion to that reported on by Chua *et al.*<sup>11</sup> Under ambipolar conditions, recombination of electrons and holes resulted in the observation of a narrow zone of light emission within the channel. The emission zone moved across the channel as the gate bias was swept during collection of the transfer data.

To fabricate the devices, a heavily doped  $n$ -type silicon wafer was used as the gate electrode. The gate electrode was coated with 400 nm of silicon nitride ( $\text{SiN}_x$ ) deposited by plasma-enhanced chemical vapor deposition. The  $\text{SiN}_x$  surface was cleaned by sonication in acetone followed by an isopropanol rinse and further sonication in isopropanol. The device was then rinsed with isopropanol and dried under a stream of  $\text{N}_2(\text{g})$ . The  $\text{SiN}_x$  was passivated with a thin film of polypropylene-co-1-butene, 14 wt % 1-butene (PPcB), see Fig. 1(b).

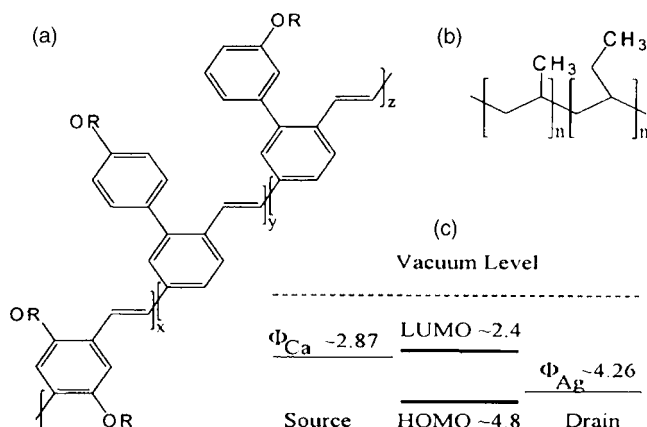


FIG. 1. Molecular structure of (a) SY and (b) PPcB. (c) Energy level diagram (units in eV) for the Ca source electrode/SY/Ag drain electrode device structure.

<sup>a)</sup> Author to whom correspondence should be addressed; electronic mail: jswensen@engineering.ucb.edu

<sup>b)</sup> Also at: Department of Physics, Center for Polymers and Organic Solids, University of California, Santa Barbara, Santa Barbara, California 93106.

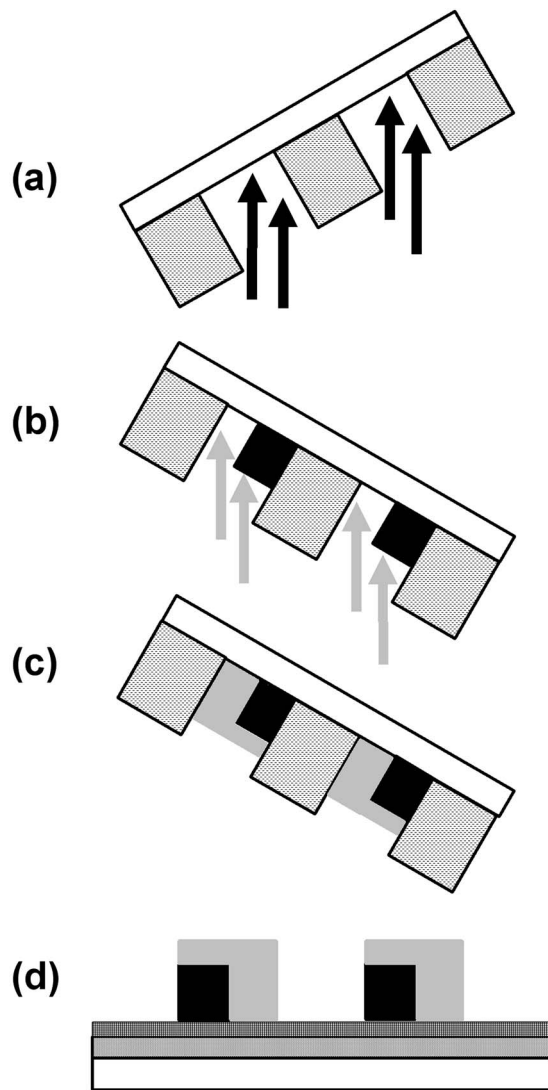


FIG. 2. Schematic of the fabrication of the top-contact two-color electrode geometry by the angled evaporation technique: (a) The substrate is mounted on a silicon shadow mask at an angle to the metal sources, and the first metal, Ca, is evaporated; (b) The angle of the mask is changed with an electric motor, and the second metal, Ag, is evaporated; (c) The deposition of the two-color electrodes is complete; and (d) Final structure of the two-color LEFET after the removal of the silicon shadow mask.

PPcB was obtained from Aldrich and used as received. 20 mg of PPcB were dissolved in 1 mL decaline at 190 °C. The substrate was placed on a spin coater preset at 2500 rpm. The PPcB solution (at 190 °C) was deposited onto the substrate. As soon as the PPcB solution covered the whole surface, the spin coater was turned on for 60 s. Uniform, 100 nm films of PPcB were obtained (thickness determined by Dektak profilometry). After transferring the coated substrate into a nitrogen glove box, the PPcB film was then dried at 200 °C for 3 min.. “SuperYellow” (SY), a polyphenylenevinylene (PPV) derivative obtained from Covion [see Fig. 1(a)], was spin cast onto the substrate at 3000 rpm. After the film deposition, the multilayer samples were annealed at 200 °C for 30 min.. The calculated capacitance of for the PPcB/SiN<sub>x</sub> gate dielectric was 9 nF/cm<sup>2</sup>.

The samples were mounted onto a silicon shadow mask in preparation for the angled evaporation technique described below. Using the angled evaporation, Ca ( $\Phi_{\text{Ca}} \sim 2.87$  eV) and Ag ( $\Phi_{\text{Ag}} \sim 4.26$  eV) were deposited during the same

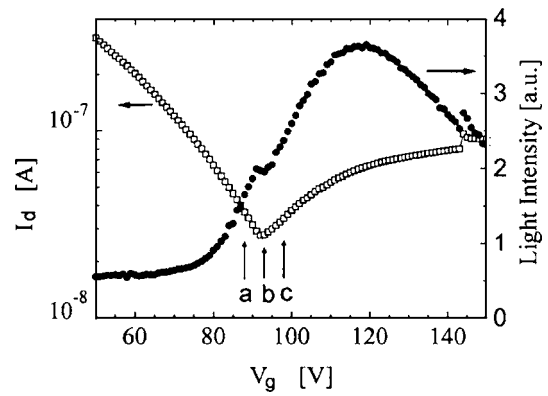


FIG. 3. Transfer scan ( $I_d$  vs  $V_g$ ) for the SY LEFET along with the corresponding emitted light intensity vs  $V_g$ . The emission zone is located in the channel: (a) Near the Ca source electrode, (b) near the center of the channel, and (c) near the Ag drain electrode (see Fig. 4).

pump down at  $\sim 1 \times 10^{-6}$  Torr to create the two-color electrode geometry. The resulting energy level diagram for SY is shown in Fig. 1(c).

The devices were tested using a Signatone probing station that is housed in a nitrogen glove box. The oxygen count was  $\sim 1.5$  ppm during device testing. A Keithley 4200 Semiconductor Characterization System was used to gather the electrical data, while light emission was collected simultaneously with a Hamamatsu photomultiplier. For each run, the Ca electrode was always negative with respect to the Ag electrode. The channel region was imaged by focusing a Pulnix charge coupled device camera on the channel through a 40 $\times$  magnification microscope objective.

The top-contact two-color electrode geometry was realized by developing a new angled evaporation technique using a silicon shadow mask. The shadow mask was fabricated by etching two parallel rectangles (1000  $\times$  100  $\mu\text{m}$ ) through a silicon wafer (250  $\mu\text{m}$  thick) separated by a 20  $\mu\text{m}$  “beam.” The rectangles defined the electrode area, while the beam defined the channel region. As shown in Fig. 2, by evaporating at an angle, the shadow created by the beam enabled the fabrication of the top contact two-color electrode geometry. The devices reported on in this work had a 16  $\mu\text{m}$  channel length and a 1000  $\mu\text{m}$  channel width. Channel lengths less than 5  $\mu\text{m}$  have been achieved with this technique.

Figure 3 shows transfer data ( $I_d$  versus  $V_g$  scan) for the LEFET, together with the gate dependence of the light emission. The transfer scan was run with a constant drain voltage ( $V_d$ ) of 200 V. The low-work-function source electrode (Ca) was grounded and the gate voltage ( $V_g$ ) was swept from 0 to 200 V. When  $V_g=0$ , there is no voltage drop between the source and gate. There is, however, a 200 V drop between the drain and gate which polarizes the gate dielectric and induces a hole channel in the vicinity of the high-work-function drain electrode (Ag). The current in this region (at lower  $V_g$  values) of the transfer scan is hole dominated.

As  $V_g$  increases, the voltage drop between the drain and gate decreases, causing the magnitude of the hole current to decrease. Simultaneously, the voltage drop between the source and the gate increases, but is oppositely charged, causing the gradual buildup of an electron channel near the low-work-function source electrode (Ca). At about  $V_g=90$  V,  $I_d$  reaches a minimum and then begins to increase again. This is the crossover point from hole-dominated cur-

rent to electron-dominated current. Crossover is expected to occur at  $V_g = \frac{1}{2} V_d$ , in good agreement with the data in Fig. 3.

Using standard FET analysis,<sup>12</sup> the field effect mobility ( $\mu$ ) can be calculated from the saturation regime of the transfer characteristics from the equation for the drain current,  $I_d = \mu C_i^* 2W/L^* (V_g - V_{th})^2$ , where  $C_i$  is the capacitance of the gate dielectric,  $V_{th}$  is the threshold voltage,  $W$  is the channel width, and  $L$  is the channel length. The resulting hole and electron mobilities are  $\mu_h = 3 \times 10^{-4} \text{ cm}^2 \text{ V s}$  and  $\mu_e = 6 \times 10^{-5} \text{ cm}^2 \text{ V s}$ . The electron mobility is lower than the hole mobility, which is likely due to residual electron traps that are still present after the PPcB passivation.

The light intensity data corresponding to the transfer scan is also shown in Fig. 3. The light intensity data begin increasing around 80 V while hole current still dominates, reaching a maximum around 120 V, well into the electron-dominated current regime. By employing the two-color electrode geometry, light emission should be observed when both electron and hole currents are simultaneously present during device operation, consistent with the light intensity versus  $V_g$  data in Fig. 3. At the crossover point, the hole and electron currents are nearly equal to each other, and the quantum efficiency for light emission is maximum. Note, however, that the light intensity peaks at  $V_g \sim 120 \text{ V}$ , i.e., when the electron current is greater than the hole current. A higher electron current might be necessary to achieve maximum brightness because the higher density of electron traps would reduce the number of electrons available for recombination.

The images taken of the channel region during operation show the location and width of the emission zone. The emission was found to be in a very narrow region ( $< 2 \mu\text{m}$ ) within the channel. The emission zone is not stationary within the channel, but in fact moves from the source to the drain as the gate voltage is swept from 88 V (a) to 93 V (b) to 98 V (c) in Fig. 3. Shown in Fig. 4 are photographs which image the position of the emission zone corresponding to points a, b, and c in Fig. 3. In Fig. 4(a), the emission zone is close to the calcium source electrode. As  $V_g$  increases, the emission moves across the channel [Fig. 4(b)], finally approaching the silver drain electrode [Fig. 4(c)]. This gate-induced shift in the emission zone from the source to the drain takes place over a small voltage range near the current crossover point. The emission line is near the center of the channel at the point where current crossover occurs.

The capacitance of the gate dielectric,  $9 \text{ nF/cm}^2$ , is relatively small. In order to increase the brightness of the emission from an LEFET, a higher gate dielectric capacitance is needed. This can be achieved by using a thinner dielectric film and/or increasing the dielectric constant of the gate dielectric.

In conclusion, an ambipolar polymer LEFET using the top contact, two-color electrode geometry (Ca as source and Ag as drain) has been demonstrated. Direct imaging of the emission zone within the channel region showed emission in a narrow region within the channel. The location of the emission zone is controlled by the gate bias. The emission zone is near the center of the channel at the crossover point where

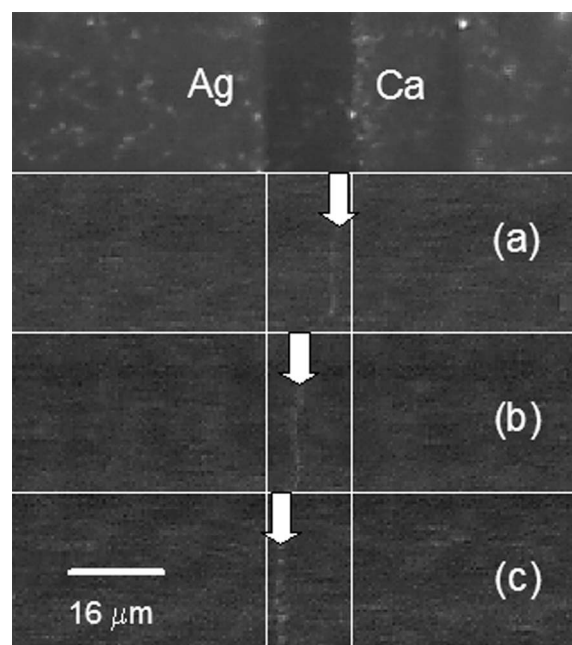


FIG. 4. The top photograph shows the Ag and Ca electrodes and the channel of the two-color LEFET. Photographs (a), (b), and (c) are taken in the dark while the device is operating. The emission zone moves from near the Ca electrode, (a)  $V_g = 88 \text{ V}$ , to midchannel, (b)  $V_g = 93 \text{ V}$ , and then approaches the Ag electrode, and (c)  $V_g = 98 \text{ V}$ .

the electron and hole currents are equal. The gate bias induced shift in the emission zone, coupled with the ambipolar charge transport, indicates that the device is truly a light-emitting transistor.

Research supported by the Air Force Office of Scientific Research (FA9550-05-0139, Charles Lee, Program Officer) and the National Science Foundation (DMR 0099843). One of the authors (J.S.) thanks Professor J. Kanicki for advice and encouragement.

<sup>1</sup>A. Hepp, H. Heil, W. Weise, M. Ahles, R. Schmechel, and H. von Seggern, *Phys. Rev. Lett.* **91**, 157406 (2003).

<sup>2</sup>C. Santato, R. Capelli, M. A. Loi, M. Murgia, F. Cicoira, V. A. L. Roy, P. Stallinga, R. Zamboni, C. Rost, S. Karg, and M. Muccini, *Synth. Met.* **146**, 329 (2004).

<sup>3</sup>C. Rost, S. Karg, W. Riess, M. A. Loi, M. Murgia, and M. Muccini, *Synth. Met.* **146**, 237 (2004).

<sup>4</sup>T. Oyamada, H. Sasabe, C. Adachi, S. Okuyama, N. Shimoji, and K. Matsushige, *Appl. Phys. Lett.* **86**, 093505 (2005).

<sup>5</sup>C. Santato, I. Manunza, A. Bonfiglio, F. Cicoira, P. Cosseddu, R. Zamboni, and M. Muccini, *Appl. Phys. Lett.* **86**, 141106 (2005).

<sup>6</sup>J. Reynaert, D. Cheyns, D. Janssen, R. Muller, V. I. Arkhipov, J. Genoe, G. Borghs, and P. Heremans, *J. Appl. Phys.* **97**, 114501 (2005).

<sup>7</sup>M. Ahles, A. Hepp, R. Schmechel, and H. von Seggern, *Appl. Phys. Lett.* **84**, 428 (2004).

<sup>8</sup>J. Swensen, D. Moses, and A. J. Heeger, in *Proceedings of the 2004 International Conference on Synthetic Metals* (University of Woolongong, Woolongong, 2004).

<sup>9</sup>T. Sakanoue, E. Fujiwara, R. Yamada, and H. Tada, *Chem. Phys. Lett.* **34**, 494 (2005).

<sup>10</sup>J. Swensen, D. Moses, and A. J. Heeger, *Synth. Met.* **153**, 53 (2005).

<sup>11</sup>L. L. Chua, J. Zausseil, J. F. Chang, E. C. W. Ou, P. K. H. Ho, H. Sirringhaus, and R. H. Friend, *Nature (London)* **434**, 194 (2005).

<sup>12</sup>S. M. Sze, *Physics of Semiconductor Devices* (Wiley, New York, 1981).